Lab on a Chip

PAPER

View Article Online
View Journal

Cite this: DOI: 10.1039/d5lc00341e

In situ electrochemical measurement of alkaline phosphatase activity in engineered gut models using a porous membrane electrode device†

Yoshinobu Utagawa,[a] Takeo Miyake,[b] Yasuhiko Shinoda,[c] Masateru Yamazaki,[c] Hiroya Abe,[ad] Hitoshi Shiku*[a] and Kosuke Ino*[a]

Received 9th April 2025,
Accepted 23rd May 2025

DOI: 10.1039/d5lc00341e

rsc.li/loc

In vitro assays utilizing human cells have attracted attention as alternatives to animal testing for drug screening. Microphysiological systems (MPS) have been proposed as cell culture platforms that more closely mimic the *in vivo* microenvironment. Engineered gut models have been extensively studied using human colorectal adenocarcinoma cell lines (Caco-2 cells). Alkaline phosphatase (ALP) activity indicates Caco-2 cell differentiation and is a component of the chemical barrier that maintains intestinal barrier function. However, conventional absorbance-based methods for ALP measurement can harm cells owing to prolonged exposure to alkaline conditions (approximately 60 min). In this study, we developed an engineered gut model with a porous membrane electrode for *in situ* measurement of ALP activity. The electrochemical sensors, positioned directly beneath the cells on porous membrane electrodes, allowed for rapid short-term measurements. ALP activity was detected after a 3 min treatment through *in situ* electrochemical measurements, which indicated low cytotoxicity. Therefore, we measured ALP activity multiple times using the same device over 21 days. The proposed system offers potential for *in situ* measurement and real-time monitoring in *in vitro* organ models, including MPS devices.

Introduction

Microphysiological systems (MPS) have attracted considerable attention for their ability to reproduce *in vivo*-like microenvironments.[1] Porous membranes are widely used in cell culture devices to construct tissue interfaces and assess barrier functions,[2] making these systems valuable for drug screening. Gut models are essential for evaluating oral drugs, as these drugs are absorbed and metabolized in the gut. Engineered gut models have been developed using transwells,[3] microfluidic devices,[4] and hydrogels[5,6] to replicate gut functions and structures. Conventionally, gut models are evaluated by trans-epithelial electrical resistance (TEER) measurements,[7] which are widely used to assess the barrier function of the cell layer noninvasively. This barrier function of the cell layer is a critical indicator because intestinal epithelial cells form tight junctions. The TEER values indicate the resistance of the entire cell layer and can significantly decrease when small holes appear in the cell layer. Therefore, other biomarkers, including those for secretion, metabolism, and enzyme activity, are necessary to robustly evaluate engineered gut models.

Alkaline phosphatase (ALP) is a critical indicator of intestinal function, as it detoxifies lipopolysaccharides in the intestines, reducing their toxicity by 99%.[8] ALP also helps maintain tight junction integrity[9] and serves as a differentiation marker in human colorectal adenocarcinoma cell lines (Caco-2 cells).[10–12] Thus, determining ALP activity in engineered gut models is essential. Typically, absorbance measurements have been widely used for ALP measurements using *p*-nitrophenyl phosphate (PNPP) as a substrate because the enzymatic product, *p*-nitrophenol (PNP), is determined by measuring the absorbance at 405 nm. Conventionally, long-term exposure (30–60 min) to alkaline conditions is necessary to accumulate enzymatic products.[13,14] The exposure damages cells because of alkaline conditions[15] and the presence of PNP,[16] resulting in impossible time-course analyses of ALP activity using the same samples. Therefore, a system that can quickly measure ALP activity is necessary to maintain cell viability after ALP measurements. To address this problem, we proposed the use of electrochemical devices for ALP assays

[a] Graduate School of Engineering, Tohoku University, Sendai 980-8579, Japan. E-mail: hitoshi.shiku.c3@tohoku.ac.jp, kosuke.ino@tohoku.ac.jp
[b] Graduate School of Information, Production and Systems, Waseda University, Kitakyushu 808-0135, Japan
[c] Organic Device Development Department, Material Development Division, Toyoda Gosei Co., Ltd., Ama 490-1207, Japan
[d] Frontier Research Institute for Interdisciplinary Sciences, Tohoku University, Sendai 980-0845, Japan

† Electronic supplementary information (ESI) available. See DOI: https://doi.org/10.1039/d5lc00341e

in which electrochemical sensors are integrated into porous membrane cell culture scaffolds, thereby eliminating the need for enzymatic product accumulation.

Electrochemical measurements are advantageous for cell analysis owing to their high sensitivity, real-time capabilities, and suitability for *in situ* applications. Integrated MPS platforms with porous membranes have been developed for various cell analyses.[17] ALP has also been measured using electrochemical techniques.[18,19] For instance, ALP serves as a biomarker of stem cell differentiation and its endogenous activity has been evaluated *via* electrochemical detection using scanning electrochemical microscopy[20] and electrode array devices.[21,22] Furthermore, the ALP activity of osteoblasts in 3D cell cultures has been measured *in situ* using electrochemical methods.[23] Although absorbance-based ALP measurements have been reported for gut models utilizing porous and thin membranes,[24] to our knowledge, few studies have focused on electrochemical measurements of ALP in gut models using porous membranes, even though ALP activity is a key indicator in oral drug evaluation. Thus, integrating electrochemical sensors within cell culture scaffolds is critical for rapid detection to reduce the incubation time.

In this study, we propose an *in situ* electrochemical measurement of ALP activity in engineered gut models using a porous membrane electrode device. Our porous membrane electrode devices function as both electrochemical sensors and cell culture scaffolds, and have previously been used to measure nitric oxide release in vascular models[25] and glucose uptake in cancer models.[26] These devices were fabricated by sputtering Au onto porous membranes; however, for this study, we selected electroless plating owing to its ability to form uniform metal layers on complex structures, including porous membranes, without requiring sputtering equipment. First, a device for sensing and cell culturing was fabricated and electrochemically evaluated. Subsequently, Caco-2 cells were cultured on a porous membrane electrode, and ALP activity was measured after 3 min of treatment using a solution containing enzymatic substrates. ALP activity was measured over 21 days using the same device. Additionally, TEER measurements were conducted to assess the impact of the electrode on TEER values. Finally, changes in ALP activity following drug treatment were evaluated.

Materials and methods

Device fabrication

Electroless Au-plated porous polycarbonate membrane electrodes were purchased from Hynts Tech Corporation (Japan). Polydimethylsiloxane (PDMS) chambers (Φ 4 mm) were fabricated in the same manner as described and then plasma-treated alongside the porous membrane electrode to adhere to both components.[25] The electrode area was 0.251 cm^2 because both sides are electrodes. Porous polyurethane membranes were obtained from Toyoda Gosei Co., Ltd. (Japan). Porous membrane electrodes were fabricated through sputtering (Ti, Pt, and Au at 200 W for 1, 0.5, and 2 min, respectively).

Electrochemical measurements

A three-electrode system, comprising a porous membrane electrode, Ag/AgCl (sat. KCl) reference electrode, and a Pt counter electrode connected to a potentiostat (HA1010 mM4, Hokuto Denko, Japan), was used (Fig. S1†). The electrochemical characteristics of the porous membrane electrodes were analyzed using a ferrocenemethanol (FMA, Tokyo Chemical Industry Co., Japan) solution. For ALP activity, 1 mM *p*-aminophenyl phosphate (PAPP, Sigma-Aldrich, USA; LKT Laboratories, Inc., USA) or 1 mM *p*-aminophenol (PAP, Wako Pure Chemical Industries, Ltd., Japan) was dissolved in a solution prepared by mixing Tris–HCl (pH 9) and Dulbecco's modified Eagle's medium (DMEM, without phenol red, Nacalai Tesque Inc., Japan) at a 1 : 1 volume ratio, with cyclic voltammetry used to identify the oxidation potential of PAP. ALP (56 500 U mL^{-1}, Oriental Yeast Co., Ltd., Japan) was added to PBS, and 10 μL of the solution was cast on the electrode (0.126 cm^2). After drying at room temperature, the device was washed twice with PBS and used for measurements. A Tris–HCl and DMEM mixture containing 4.7 mM PAPP was added to the device, and the device was treated at 37 °C for 3 min. After the treatment, amperometry was performed.

Cell culture

Caco-2 cells (RIKEN BRC., Japan) were cultured in DMEM (Nacalai Tesque Inc.) supplemented with 10% fetal bovine serum (Gibco, USA), 1% penicillin–streptomycin (Gibco), and 1% nonessential amino acids (NEAA, Gibco). The cells were maintained in a humidified atmosphere containing 5% CO_2 at 37 °C.

Live/dead staining

For viability analysis, Caco-2 cells cultured on the device were treated with a Double Staining Kit (Dojindo, Japan) for 30 min at 37 °C. Calcein AM and PI staining in the cells were imaged on a microscope (ECLIPSE Ti2, Nikon, Japan) with exposure times of 50 ms for calcein AM and 100 ms for PI at 470 and 525 nm, respectively.

Cell culture on the device

Before cell seeding, the devices were sterilized by exposure to ultraviolet light for 15–30 min. To measure the ALP activity of Caco-2 cells cultured in the device, collagen type I (20 μg cm^{-2}, EMD Millipore Corp., USA) was coated onto the porous membrane electrode at 37 °C for 30 min. After coating, 20 μL of a cell suspension of Caco-2 cells (5×10^5 cells cm^{-2}) was added to the device. The cells were seeded at a confluent density to facilitate the rapid formation of tight junctions. After 2 h from seeding, 130 μL of an additional culture medium was added to the device. The culture medium was changed every 2 days.

Electrochemical measurements for ALP activity of Caco-2 cells

The devices with Caco-2 cells were washed twice with Dulbecco's phosphate-buffered saline (−) (D-PBS(−), Nacalai Tesque Inc.). Then, 150 μL (front: 140 μL, back: 10 μL) of a Tris–HCl and DMEM mixture containing 4.7 mM PAPP (pH 9) was added to each device and incubated at 37 °C for 0, 3, or 60 min. After incubation, the reference and counter electrodes were set, and electrochemical measurements were conducted.

Absorbance measurements

A Tris–HCl and DMEM mixture containing 4.7 mM *p*-nitrophenyl phosphate (PNPP, Thermo Scientific, USA) (pH 9) was prepared. The solution was added to each device and incubated at 37 °C for 3 min. After incubation, the solution was collected from the devices and analyzed using a microplate reader (iMark, BIO-RAD, USA).

TEER measurements

A PDMS insert was fabricated for TEER measurements (Fig. S2A†). Caco-2 cells were cultured on the porous membrane electrodes in the insert. First, the culture medium was transferred to a TEER measurement device (World Precision Instruments). The insert with the fresh culture medium was subsequently placed in the TEER measurement device (Fig. S2B†). The resistance values were recorded 60 s after setting. TEER measurements were performed every 2 days.

Toxicity measurements

Caco-2 cells were seeded and cultured in a 96-well plate (4×10^4 cells well^{-1}) for 2 days. Next, 100 μL of DMEM containing 0–100 μM afatinib was added to each well. After 24 h, 10 μL of the Cell Counting Kit reagent (Dojindo) was added and incubated at 37 °C for 1 h to assess cell viability. The absorbance was measured at 450 nm using a microplate reader.

Electrochemical measurements for ALP activity with afatinib treatment

Afatinib was dissolved in dimethyl sulfoxide (DMSO, Sigma-Aldrich) to prepare a 10 mM solution. The final concentration of DMSO was adjusted to remain below 1%. Caco-2 cells were cultured in the devices for 2 days and then treated with a medium containing 0, 10, or 50 μM afatinib. After 24 h, the devices were washed twice with PBS. Next, a Tris–HCl and DMEM mixture containing 4.7 mM PAPP (pH 9) was added to the device and incubated at 37 °C for 3 min. After incubation, electrochemical measurements were performed.

Results and discussion

Schematics of cell culture and electrochemical measurements

Fig. 1 depicts a schematic of the device, cell culture setup, and electrochemical measurement process for ALP activity. Porous membrane electrodes were fabricated by electroless Au plating of porous polycarbonate membranes. The device consisted of porous membrane electrodes with PDMS chambers. Caco-2 cells were cultured on collagen-coated porous membrane electrodes, with the electrochemical sensors positioned near the cells using the porous membrane electrodes. For the electrochemical measurements of ALP activity, PAPP was used as an enzymatic substrate, generating PAP through ALP activity. PAP may diffuse not only between cells but also inside cells because PAP is a small and moderately polar molecule. Subsequently, PAP was oxidized on the porous membrane electrode by applying a voltage of +0.3 V. In this study, PAPP is converted to PAP on the ALP expressed in the apical membranes of Caco-2 cells. The generated PAP diffuses to the electrode.

Characterization of porous membrane electrode

Fig. 2A depicts an image of the fabricated device. The electroless plating coated both sides of the porous membrane with Au, which could result in mixed signal information when cells were cultured on both sides. Although not conducted in this study, this issue can be addressed by etching one side of the membrane.[27] The scanning electron microscopy (SEM) image of

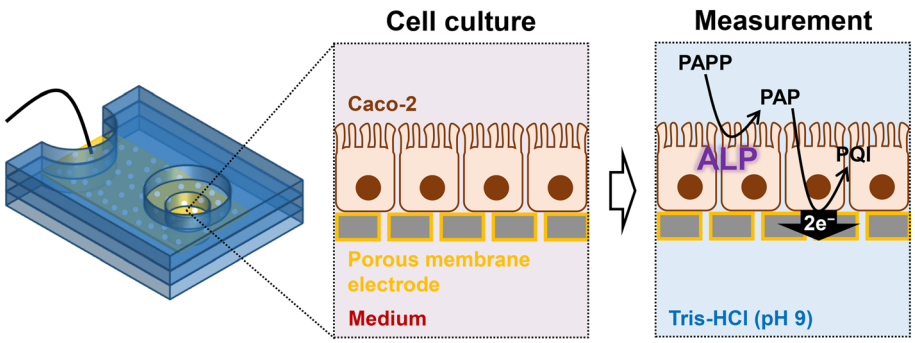

Fig. 1 Schematic illustration of cell culture and electrochemical measurements on the porous membrane electrode.

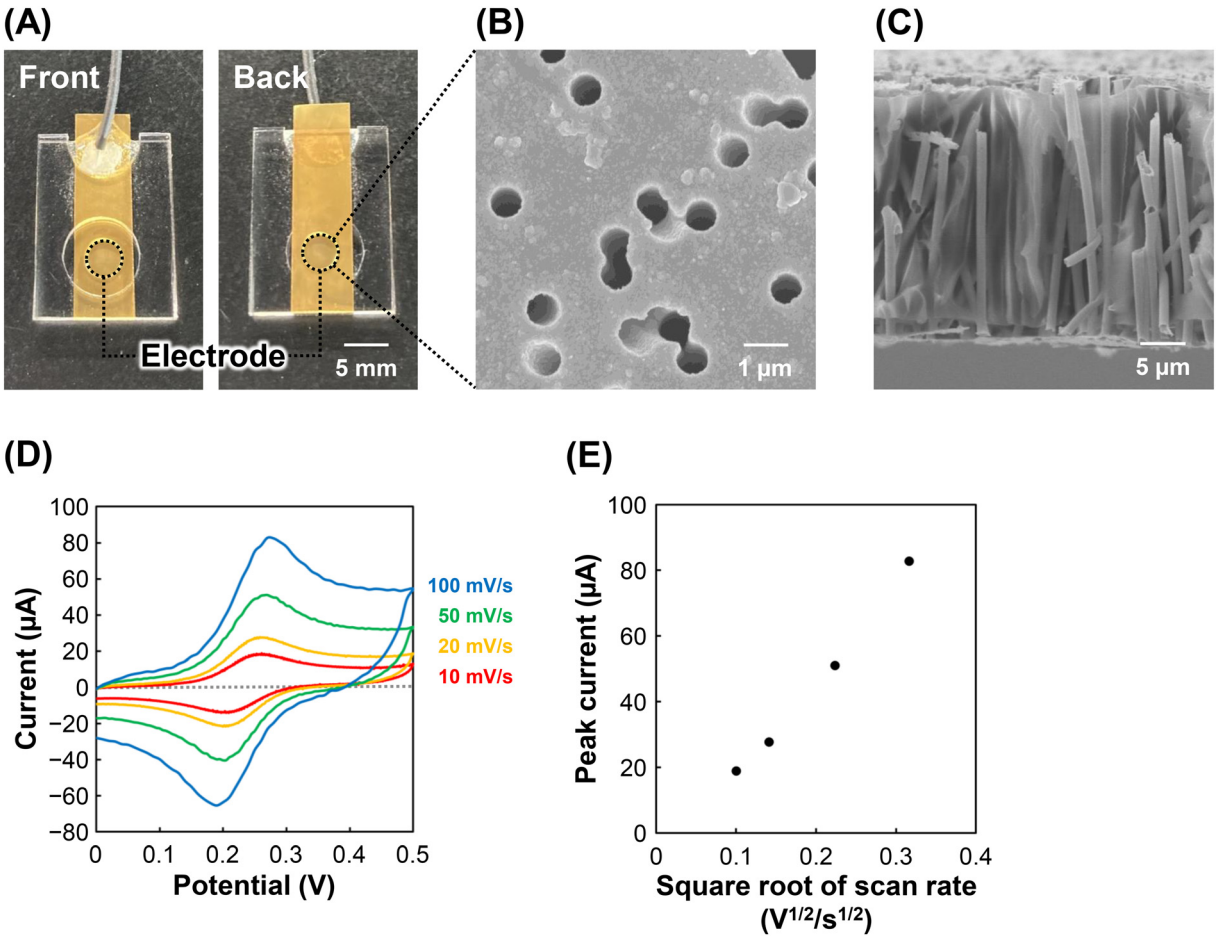

Fig. 2 Characterization of porous membrane electrodes. (A) Photograph of the device. (B and C) Scanning electron microscopy (SEM) images showing the (B) surface and (C) cross section. (D) Cyclic voltammograms of 1 mM FMA at scan rates of 10–100 mV s^{-1}. (E) Relationship between peak current *vs.* square root of the scan rate.

the device surface reveals a pore size of 1 μm and a pore density of 2.2×10^7 pores cm^{-2} (Fig. 2B). The SEM cross-section image indicates that the porous membrane electrode has an approximate thickness of 27 μm. Additionally, tube structures were observed (Fig. 2C), such structures are not seen in track-etched membranes.[28] Therefore, the observed tube structures correspond to the Au formed within the pores.

Cyclic voltammetry was conducted using this device, with peak currents of FMA increasing in proportion to the scan rate (Fig. 2D). The ΔE_p value was 70 mV at a scan rate of 50 mV s^{-1}, indicating clean electrode surfaces. Additionally, the peak currents were linearly related to the square root of the scan rate (Fig. 2E), indicating a diffusion-controlled reaction. The porous membrane electrode demonstrated reproducibility and stability as an electrochemical sensor.

Electrochemical measurements of PAP using a porous membrane electrode device

ALP converts PAPP into PAP, which can then be quantified by oxidizing PAP on the electrode. A mixture of Tris–HCl buffer and DMEM (pH 9) was used as the measurement solution to suppress the oxidative polymerization of PAP, thus preventing additional oxidation currents from polymer formation (Fig. S3†). This may be due to the antioxidant effect of pyruvate contained in the medium. Fig. 3A shows the cyclic voltammograms of PAP, PAPP, and the buffer. The oxidation peak for PAP was observed at +0.05 V, whereas the oxidation peak for PAPP appeared at +0.5 V. For this study, +0.3 V was selected for PAP measurement to ensure the oxidation of PAP without affecting PAPP. Additionally, PAP is fully oxidized at +0.3 V even with electrode fouling. Fig. 3B shows amperograms obtained at different PAP concentrations, where the potential was stepped from −0.1 to +0.3 V at 10 s. The oxidation current at 20 s corresponded to the PAP concentration, showing a linear relationship (Fig. 3C). Fig. 3D illustrates amperograms using electrodes cast with ALP, with the oxidation current corresponding to the amount of ALP (Fig. 3E). Thus, this device allows ALP activity to be measured *via* PAP oxidation.

ALP activity measurements of Caco-2 cells

The ALP activity of the Caco-2 cells was confirmed through optical and electrochemical measurements. In the optical

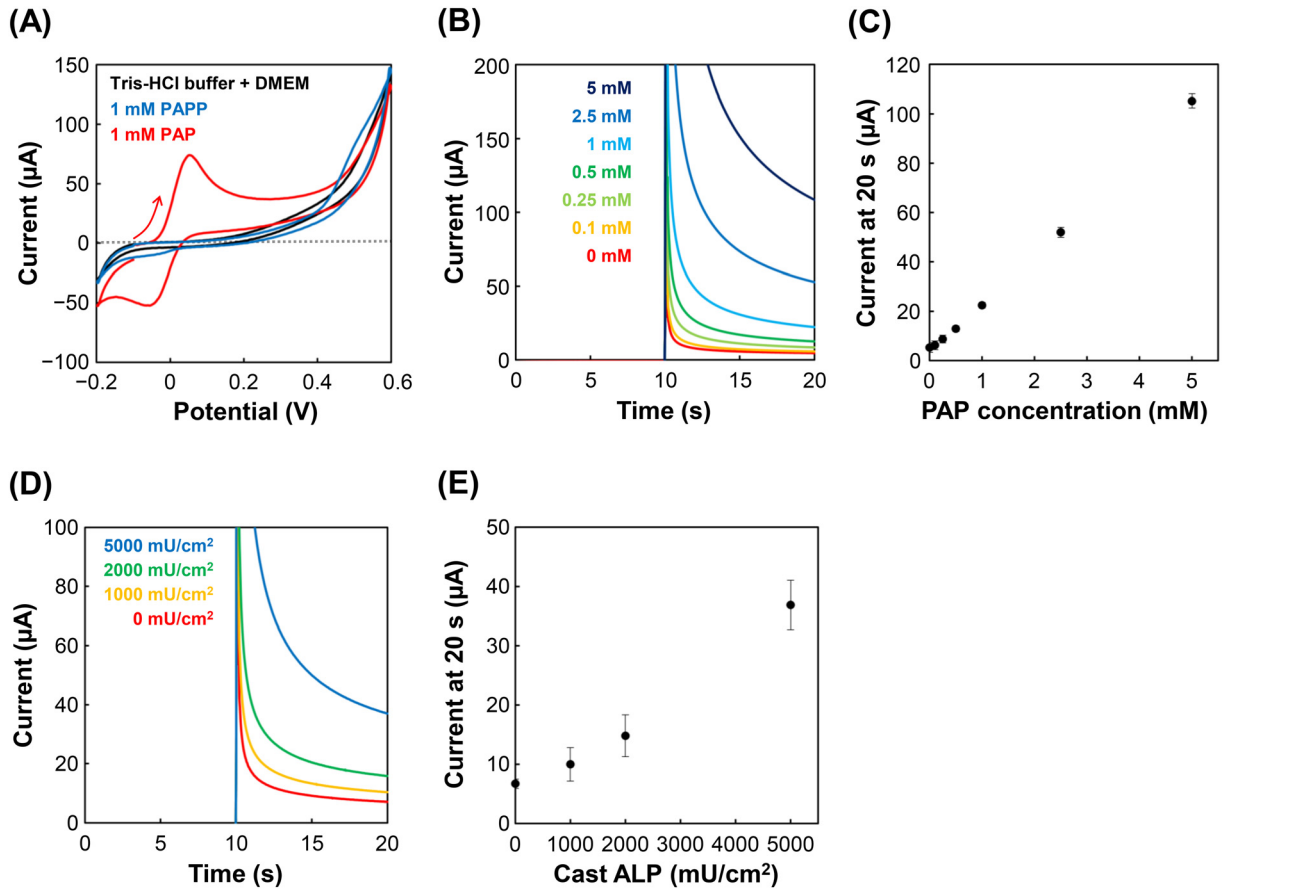

Fig. 3 Electrochemical measurement for PAP. (A) Cyclic voltammograms of 1 mM PAP, 1 mM PAPP, and Tris–HCl buffer at a scan rate of 50 mV s^{-1}. (B) Amperograms of PAP at concentrations of 0–5 mM. (C) Calibration curve for PAP (n = 3). (D) Amperograms of PAP generated from 4.7 mM PAPP with cast ALP of 0–5000 mU cm^{-2} after 3 min of incubation. (E) Calibration curve of ALP (n = 3). Error bars indicate standard deviations.

method, the absorbance of the Caco-2 cells was higher than that of the cell-free and human umbilical vein endothelial cell controls (Fig. S4A†). Similarly, electrochemical measurements using a Au disk electrode yielded the same results (Fig. S4B†). Thus, ALP activity in Caco-2 cells was verified, and an electrochemical method was applied for measurement.

Subsequently, ALP activity was evaluated using a porous membrane electrode device cultured with Caco-2 cells. After 2 days of culture, cells proliferated within the device (Fig. S5A†). Subsequently, the ALP activity was measured with a 3 min treatment. Since Mg^{2+} activates ALP, the effect of Mg^{2+} concentration was investigated. The Tris–HCl and DMEM mixture initially contained 0.4 mM Mg^{2+}, while a previous study used 2 mM Mg^{2+} for ALP activation.[29] As a result, no significant difference in ALP activity was observed between 0.4 and 2 mM Mg^{2+} (Fig. S5B†); thus, a 0.4 mM Mg^{2+} solution was used because no additional reagents were required. Additionally, cytotoxicity by measurement solution was investigated. A 60 min treatment at pH 9 caused cell detachment (Fig. S5C†). In contrast, a 3 min treatment with 4.7 mM PAPP at pH 9 did not affect cell morphology and metabolism (Fig. S5C and D†).

When collagen-coated devices without cells were used, the oxidation current did not increase even after 60 min of treatment (Fig. 4A). In contrast, an increase in oxidation current was observed when using devices cultured with Caco-2 cells for 2 days (Fig. 4A), indicating successful *in situ* measurement of ALP activity with the porous membrane electrodes. Longer treatment times generated more PAP, resulting in higher current values (Fig. 4B). ALP activity was detected immediately after the measurement solution was added, demonstrating that this system enabled rapid measurements. However, a 3 min treatment was chosen for this study owing to the manual effort involved in changing solutions and preparing devices. ALP activity in the Caco-2 cells increased with culture time, as ALP was generated on the apical side of the Caco-2 cells during differentiation.[30] After each measurement, Caco-2 cells were cultured continuously, allowing ALP activity to be measured with the same samples (Fig. 4C). The first current response at day 2 was used as a standard, and changes in the current values in subsequent measurements were analyzed. When measured after the 3 min treatment, the normalized current increased, whereas 60 min treatments led to a decrease, suggesting cell damage from prolonged exposure to alkaline conditions (pH 9) (Fig. S5E†). Therefore, rapid measurements are essential to minimize cell damage.

The effects of multiple measurements on ALP levels were next assessed (Fig. 4D). The current values from devices that

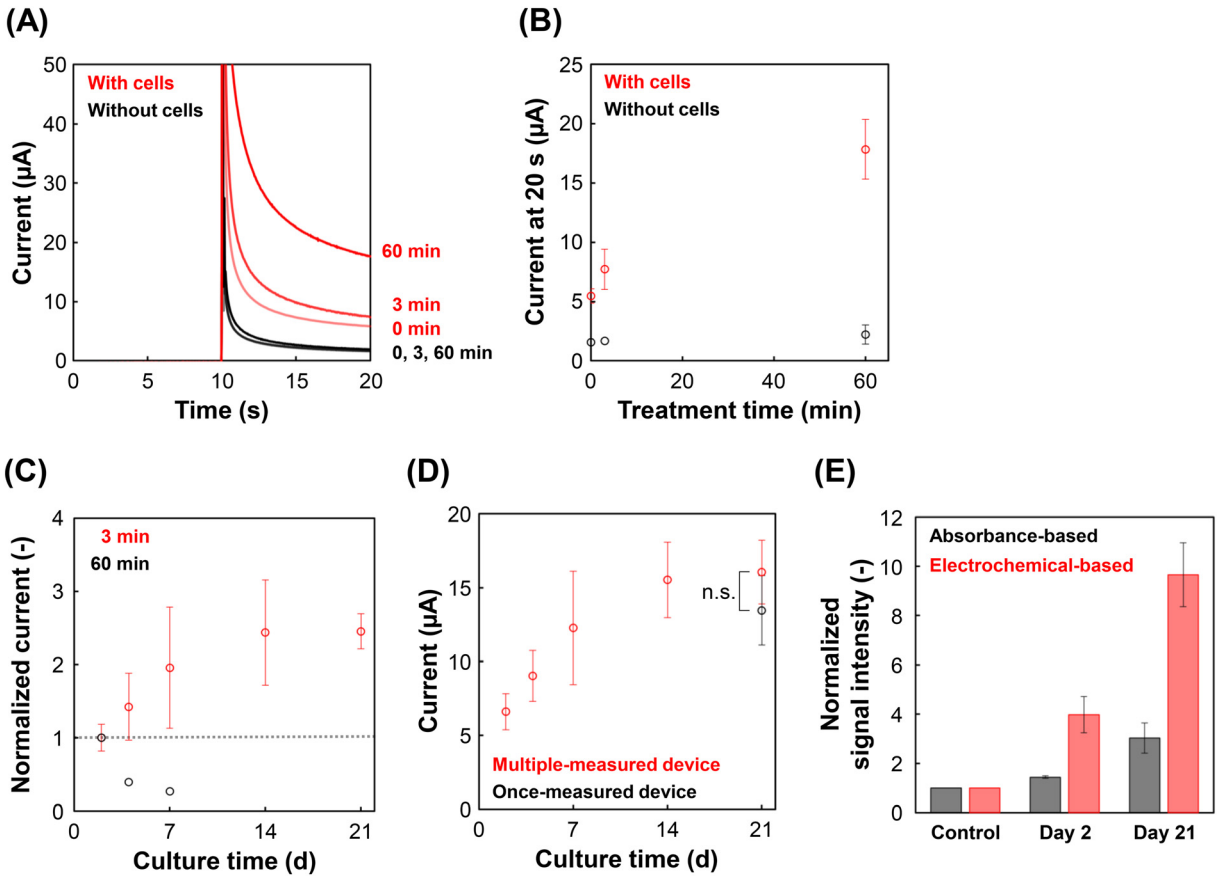

Fig. 4 ALP activity measurements of Caco-2 cells cultured on the device. (A) Amperograms showing ALP activity measurements. The devices were treated with Tris–HCl buffer containing 4.7 mM PAPP for 0, 3, or 60 min. (B) Plots of oxidation current at 20 s, with or without Caco-2 cells (n = 1–8). (C) Normalized currents across different culture days, where cells were treated with a solution containing 4.7 mM PAPP for 3 or 60 min (n = 1–3). (D) Plots of oxidation current over culture days (n = 3). (E) Normalized absorbances and currents on day 2 and day 21 based on the cell-free condition (n = 1–3). Error bars indicate standard deviations. Student's t-tests were performed.

underwent multiple measurements were similar to those measured only once, indicating that 3 min exposure to alkaline conditions and electrochemical measurements did not affect subsequent ALP readings. Live/dead staining further confirmed cell viability, with most Caco-2 cells remaining viable under both conditions (Fig. S5F†).

In addition to *in situ* electrochemical measurements, absorbance measurements using a PNPP-containing solution were performed on day 2 and day 21 with a device cultured with Caco-2 cells. Both absorbance and electrochemical signals increased compared to the cell-free condition (Fig. 4E). The electrochemical measurements exhibited a larger increase, whereas *in situ* measurements demonstrated higher sensitivity. Therefore, further reductions in measurement time can be expected by using a microfluidic system integrated with a porous membrane electrode.

TEER measurements

To determine if TEER measurements could be performed with porous membrane electrodes, TEER was measured for the Caco-2 cells cultured on these electrodes. Measurements were taken every 2 days (Fig. 5). The TEER values initially increased until day 4, then decreased to approximately 100 Ω cm^2 on day 6 before increasing again, reaching 350 Ω cm^2 on day 21. These values fall within a reasonable range (150–400 Ω cm^2) for TEER in Caco-2 models using non-conductive

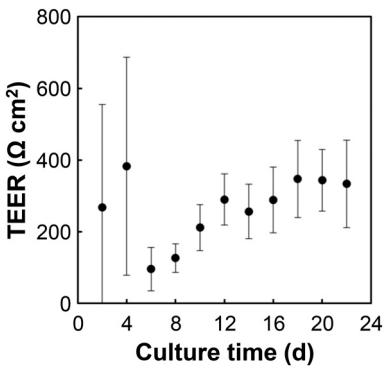

Fig. 5 TEER measurements for Caco-2 cells cultured on the porous membrane electrode from day 2 to day 22 (n = 6). Error bars represent standard deviations.

porous membranes.[31,32] Furthermore, the trend in the undulating TEER values was consistent with that of previously reported patterns, potentially reflecting changes in junctional length during culture.[33] From these results, porous membrane electrodes can be effectively used for TEER measurements in addition to porous membranes. In our study, both TEER values and ALP activity remained constant between day 14 and day 21. TEER values showed more variability in early culture stages, whereas ALP activity remained comparatively stable, indicating that it might serve as a useful evaluation indicator in short-term cultures. TEER measurements, however, can be conducted directly in the medium, unlike ALP activity measurements, which require an alkaline solution and enzymatic substrates, which are disadvantageous under some conditions.

ALP activity measurements with drug treatment

Afatinib, an oral anticancer drug and epidermal growth factor receptor inhibitor, has been shown in previous studies to reduce TEER values in intestinal epithelial models.[34,35] Although several studies suggest a potential involvement of ALP in maintaining intestinal barrier function,[9,36] its response to afatinib in engineered gut models has not been previously examined.

To assess cytotoxicity, afatinib was first tested in 96-well plates. Changes in cell morphology were observed at concentrations above 50 μM (Fig. S6A†), with a noticeable decrease in cell viability at 50 μM and cell death predominating at 100 μM (Fig. S6B†). Subsequently, ALP activity was measured electrochemically after treating Caco-2 cells with afatinib. Cells cultured for 2 or 7 days were exposed to afatinib for 24 h, after which ALP activity was measured. After 2 days of culture, the oxidation current remained unchanged with 10 μM afatinib but significantly decreased at 50 μM (Fig. 6). Dimethyl sulfoxide did not affect ALP activity (Fig. S7†), which is consistent with toxicity tests (Fig. S6B†). This indicates that 2 days of culture may be insufficient for drug assessment, as 10 μM afatinib—effective in reducing barrier function[35]—did not reduce ALP activity. However, for cells cultured for 7 days, ALP activity decreased even with 10 μM afatinib, suggesting that drug evaluation using this system requires at least 7 days of culture. The increasing ALP synthesis rate in differentiated Caco-2 cells[10] may explain why 2-day cultures show less sensitivity to afatinib at lower concentrations (10 μM)—detecting changes after a 2-day culture might be difficult owing to the low synthesis rate of ALP, whereas a 7-day culture, with increased ALP synthesis, exhibits detectable activity changes.

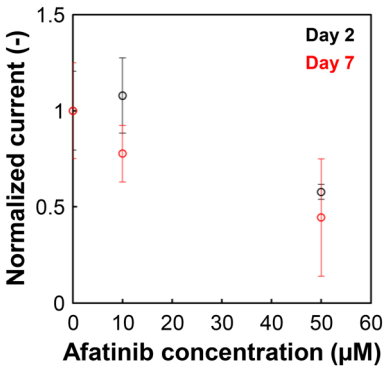

Fig. 6 Electrochemical measurements of ALP activity following afatinib treatment. Oxidation currents for various afatinib concentrations on day 2 and day 7 (n = 3–8). Error bars indicate standard deviations.

The effects of different scaffold structures on the ALP activity of Caco-2 cells were also examined.[37] Previously, a glucose sensor using a porous polyurethane membrane electrode with asymmetric pores was reported.[26] The surfaces of the porous membranes were uneven compared with those of the track-etched membranes. Therefore, the effects of different scaffold structures on the ALP activity were investigated. First, the electrochemical measurements of PAP were performed using polyurethane membranes (Fig. S8†). Fig. S9A† illustrates the ALP activity under varying culture days with the porous polyurethane membrane electrodes. The currents in the polyurethane membranes increased considerably on day 4, indicating that the membrane structure might facilitate ALP expression. From day 7 to day 21, the current values stabilized. In this study, we successfully evaluated ALP activity in engineered gut models using porous polyurethane membrane electrodes. Most Caco-2 cells remained viable after multiple measurements on polyurethane scaffolds, demonstrating the viability of the method for long-term measurements (Fig. S9B†).

We developed a system that could measure ALP activity quickly and with lower cytotoxicity because evaluating ALP activity is critical in an engineered gut model. The results revealed that the porous membrane electrode devices allowed the evaluation of ALP activity after a 3 min treatment, and the method was demonstrated to be less cytotoxic. This treatment time was considerably shorter than the time required for conventional ALP activity measurements.

Porous membrane electrodes and porous membranes have been used for TEER measurements. Furthermore, porous membrane electrodes can measure the TEER[38] and be used for impedance measurements to evaluate cell adhesions, including cell–cell and cell–substrate adhesion.[39]

ALP activity measurements were performed using porous membranes comprising different materials and structures, suggesting that membranes from different materials could be used as electrode scaffolds in MPS research.[40] Electroless plating, which provides a uniform coating on complex structures, is a versatile alternative to sputtering, capable of evaluating ALP activity based on scaffold materials and structures. For instance, stretchable porous membranes could assess mechanical stimulations,[41] while asymmetric porous membranes could evaluate cell–cell interactions.[42]

Integrating porous membrane electrodes into microfluidic devices may further accelerate ALP measurements. Advanced

intestine-on-a-chip models, incorporating mucus layers on top of human intestinal cells that are co-cultured with microbiota, have been developed.[43] *In vivo* studies suggest that colonic ALP activity correlates with gut mucus functionality.[44] Thus, measuring ALP activity in complex gut models with mucus layers will be increasingly important, with the ability to perform these evaluations on a single device over extended periods adding significant value.

Conclusion

We successfully developed engineered gut models using porous membrane electrodes for rapid and efficient evaluation of ALP activity. These devices were fabricated with porous membrane electrodes, enabling Caco-2 cells to be cultured on the system for up to 21 days. ALP activity in Caco-2 cells was measured within a 3 min treatment window, significantly reducing cytotoxicity while allowing for multiple measurements over the 21 days without impacting cell culture viability or ALP activity. Additionally, the system effectively detected drug-induced changes in ALP activity, underscoring its potential as a robust platform for drug screening. This versatile system holds promise as a valuable tool in drug discovery, particularly for applications involving MPS devices.

Data availability

The datasets are available from the corresponding author upon reasonable request.

Conflicts of interest

Some of the authors (YS and MY) of this paper are employees of Toyoda Gosei Co., Ltd. (TG), and the material used in this study is a product candidate developed by TG, which it intends to commercialize. However, we have strived to ensure the utmost objectivity and fairness in the design of this study, the collection, analysis, and interpretation of data, and in writing this manuscript.

Acknowledgements

This work was supported by a Grant-in-Aid for JSPS Fellows (No. 24KJ0353), a Grant-in-Aid for Early-Career Scientists (No. 22K14707 and 24K17706), a Grant-in-Aid for Scientific Research (A) (No. 20H00619), a Grant-in-Aid for Scientific Research (B) (No. 21H01957 and 22H02102), a Grant-in-Aid for Challenging Research (Exploratory) (No. 23K17926), and a Grant-in-Aid for Scientific Research (S) (No. 24H00070) from the Japan Society for the Promotion of Science. This study was supported by AMED (No. JP22be1004205, JP23be1004205, and JP24be1004205).

References

1 D. E. Ingber, Human organs-on-chips for disease modelling, drug development and personalized medicine, *Nat. Rev. Genet.*, 2022, **23**(8), 467–491.
2 H. H. Chung, M. Mireles, B. J. Kwarta and T. R. Gaborski, Use of porous membranes in tissue barrier and co-culture models, *Lab Chip*, 2018, **18**(12), 1671–1689.
3 A. Lechanteur, A. Almeida and B. Sarmento, Elucidation of the impact of cell culture conditions of Caco-2 cell monolayer on barrier integrity and intestinal permeability, *Eur. J. Pharm. Biopharm.*, 2017, **119**, 137–141.
4 H. J. Kim, D. Huh, G. Hamilton and D. E. Ingber, Human gut-on-a-chip inhabited by microbial flora that experiences intestinal peristalsis-like motions and flow, *Lab Chip*, 2012, **12**(12), 2165–2174.
5 N. Torras, J. Zabalo, E. Abril, A. Carré, M. García-Díaz and E. Martínez, A bioprinted 3D gut model with crypt-villus structures to mimic the intestinal epithelial-stromal microenvironment, *Biomater. Adv.*, 2023, **153**, 213534.
6 D. Vera, M. García-Díaz, N. Torras, Ó. Castillo, X. Illa, R. Villa, M. Alvarez and E. Martinez, A 3D bioprinted hydrogel gut-on-chip with integrated electrodes for transepithelial electrical resistance (TEER) measurements, *Biofabrication*, 2024, **16**(3), 035008.
7 O. Y. F. Henry, R. Villenave, M. J. Cronce, W. D. Leineweber, M. A. Benz and D. E. Ingber, Organs-on-chips with integrated electrodes for trans-epithelial electrical resistance (TEER) measurements of human epithelial barrier function, *Lab Chip*, 2017, **17**(13), 2264–2271.
8 A. B. Schromm, K. Brandenburg, H. Loppnow, U. Zähringer, E. T. Rietschel, S. F. Carroll, M. H. Koch, S. Kusumoto and U. Seydel, The charge of endotoxin molecules influences their conformation and IL-6-inducing capacity, *J. Immunol.*, 1998, **161**(10), 5464–5471.
9 W. Liu, D. Hu, H. Huo, W. Zhang, F. Adiliaghdam, S. Morrison, J. M. Ramirez, S. S. Gul, S. R. Hamarneh and R. A. Hodin, Intestinal alkaline phosphatase regulates tight junction protein levels, *J. Am. Coll. Surg.*, 2016, **222**(6), 1009–1017.
10 H. Matsumoto, R. H. Erickson, J. R. Gum, M. Yoshioka, E. Gum and Y. S. Kim, Biosynthesis of alkaline phosphatase during differentiation of the human colon cancer cell line Caco-2, *Gastroenterology*, 1990, **98**(5 Pt 1), 1199–1207.
11 X. Wang, L. Li and G. Zhang, Impact of deoxynivalenol and kaempferol on expression of tight junction proteins at different stages of Caco-2 cell proliferation and differentiation, *RSC Adv.*, 2019, **9**(59), 34607–34616.
12 S. Zeiringer, L. Wiltschko, C. Glader, M. Reiser, M. Absenger-Novak, E. Fröhlich and E. Roblegg, Development and characterization of an in vitro intestinal model including extracellular matrix and macrovascular endothelium, *Mol. Pharmaceutics*, 2023, **20**(10), 5173–5184.
13 Y. Chen, Y. Lin, K. M. Davis, Q. Wang, J. Rnjak-Kovacina, C. Li, R. R. Isberg, C. A. Kumamoto, J. Mecsas and D. L. Kaplan, Robust bioengineered 3D functional human intestinal epithelium, *Sci. Rep.*, 2015, **5**, 13708.
14 K. Kulthong, L. Duivenvoorde, H. Sun, S. Confederat, J. Wu, B. Spenkelink, L. de Haan, V. Marin, M. van der Zande and H. Bouwmeester, Microfluidic chip for culturing intestinal epithelial cell layers: Characterization and comparison of

drug transport between dynamic and static models, *Toxicol. In Vitro*, 2020, **65**, 104815.
15 H. von Euler, A. Söderstedt, A. Thörne, J. M. Olsson and G. Yongqing, Cellular toxicity induced by different pH levels on the R3230AC rat mammary tumour cell line. An in vitro model for investigation of the tumour destructive properties of electrochemical treatment of tumours, *Bioelectrochemistry*, 2002, **58**(2), 163–170.
16 M. Majewska, F. Khan, I. S. Pieta, A. Wróblewska, R. Szmigielski and P. Pieta, Toxicity of selected airborne nitrophenols on eukaryotic cell membrane models, *Chemosphere*, 2021, **266**, 128996.
17 K. Ino, Y. Utagawa, K. Hiramoto, H. Abe and H. Shiku, Porous membranes integrated into electrochemical systems for bioanalysis, *Electrochem. Sci. Adv.*, 2024, e2300026.
18 H. Chen, L. Tian, X. Sun, L. Liu, R. Ma and M. Zhang, Alkaline phosphatase for estimating the time since deposition of blood fingerprints by scanning electrochemical microscopy, *Anal. Chem.*, 2023, **95**(50), 18470–18478.
19 Y. Kanno, Y. Zhou, T. Fukuma and Y. Takahashi, Alkaline phosphatase-based electrochemical analysis for point-of-care testing, *Electroanalysis*, 2022, **34**(2), 161–167.
20 Y. Matsumae, T. Arai, Y. Takahashi, K. Ino, H. Shiku and T. Matsue, Evaluation of the differentiation status of single embryonic stem cells using scanning electrochemical microscopy, *Chem. Commun.*, 2013, **49**(58), 6498–6500.
21 K. Ino, T. Nishijo, T. Arai, Y. Kanno, Y. Takahashi, H. Shiku and T. Matsue, Local redox-cycling-based electrochemical chip device with deep microwells for evaluation of embryoid bodies, *Angew. Chem., Int. Ed.*, 2012, **51**(27), 6648–6652.
22 Y. Kanno, K. Ino, H. Abe, C. Sakamoto, T. Onodera, K. Y. Inoue, A. Suda, R. Kunikata, M. Matsudaira, H. Shiku and T. Matsue, Electrochemicolor imaging using an LSI-based device for multiplexed cell assays, *Anal. Chem.*, 2017, **89**(23), 12778–12786.
23 C. Caviglia, R. P. Carletto, S. De Roni, Y. M. Hassan, S. Hemanth, M. Dufva and S. S. Keller, In situ electrochemical analysis of alkaline phosphatase activity in 3D cell cultures, *Electrochim. Acta*, 2020, **359**, 136951.
24 M. S. Jeon, Y. Y. Choi, S. J. Mo, J. H. Ha, Y. S. Lee, H. U. Lee, S. D. Park, J.-J. Shim, J.-L. Lee and B. G. Chung, Contributions of the microbiome to intestinal inflammation in a gut-on-a-chip, *Nano Convergence*, 2022, **9**(1), 8.
25 Y. Utagawa, K. Ino, K. Hiramoto, K. Iwase, Y. Nashimoto, I. Honma and H. Shiku, Vasculature-on-a-chip with a porous membrane electrode for in situ electrochemical detection of nitric oxide released from endothelial cells, *Anal. Chem.*, 2023, **95**(49), 18158–18165.
26 Y. Utagawa, K. Ino, Y. Shinoda, M. Yamazaki, H. Abe and H. Shiku, Enzyme-free in-situ electrochemical measurement using a porous membrane electrode for glucose transport into cell spheroids, *ACS Sens.*, 2024, **9**(8), 4248–4255.
27 B. Zhang, Y. Shi, D. Miyamoto, K. Nakazawa and T. Miyake, Nanostraw membrane stamping for direct delivery of molecules into adhesive cells, *Sci. Rep.*, 2019, **9**(1), 6806.
28 P. Y. Apel, I. V. Blonskaya, S. N. Dmitriev, O. L. Orelovitch and B. Sartowska, Structure of polycarbonate track-etch membranes: Origin of the "paradoxical" pore shape, *J. Membr. Sci.*, 2006, **282**(1), 393–400.
29 Y. Kanno, K. Ino, H. Shiku and T. Matsue, A local redox cycling-based electrochemical chip device with nanocavities for multi-electrochemical evaluation of embryoid bodies, *Lab Chip*, 2015, **15**(23), 4404–4414.
30 T. Nakano, I. Inoue, D. H. Alpers, Y. Akiba, S. Katayama, R. Shinozaki, J. D. Kaunitz, S. Ohshima, M. Akita, S. Takahashi, I. Koyama, M. Matsushita and T. Komoda, Role of lysophosphatidylcholine in brush-border intestinal alkaline phosphatase release and restoration, *Am. J. Physiol.*, 2009, **297**(1), G207–G214.
31 B. Srinivasan, A. R. Kolli, M. B. Esch, H. E. Abaci, M. L. Shuler and J. J. Hickman, TEER measurement techniques for in vitro barrier model systems, *J. Lab. Autom.*, 2015, **20**(2), 107–126.
32 S. Lopez-Escalera and A. Wellejus, Evaluation of Caco-2 and human intestinal epithelial cells as in vitro models of colonic and small intestinal integrity, *Biochem. Biophys. Rep.*, 2022, **31**, 101314.
33 K. Felix, S. Tobias, H. Jan, S. Nicolas and M. Michael, Measurements of transepithelial electrical resistance (TEER) are affected by junctional length in immature epithelial monolayers, *Histochem. Cell Biol.*, 2021, **156**(6), 609–616.
34 Y. Kim, A. Quach, S. Das and K. E. Barrett, Potentiation of calcium-activated chloride secretion and barrier dysfunction may underlie EGF receptor tyrosine kinase inhibitor-induced diarrhea, *Physiol. Rep.*, 2020, **8**(13), e14490.
35 T. Mehmood, R. Pichyangkura and C. Muanprasat, Chitosan oligosaccharide prevents afatinib-induced barrier disruption and chloride secretion through modulation of AMPK, PI3K/AKT, and ERK signaling in T84 cells, *Polymers*, 2022, **14**(20), 4255.
36 S. B. Singh, C. N. Coffman, M. G. Varga, A. Carroll-Portillo, C. A. Braun and H. C. Lin, Intestinal alkaline phosphatase prevents sulfate reducing bacteria-induced increased tight junction permeability by inhibiting snail pathway, *Front. Cell. Infect. Microbiol.*, 2022, **12**, 882498.
37 M. Hu, Y. Li, J. Huang, X. Wang and J. Han, Electrospun scaffold for biomimic culture of Caco-2 cell monolayer as an in vitro intestinal model, *ACS Appl. Bio Mater.*, 2021, **4**(2), 1340–1349.
38 C. Pitsalidis, D. van Niekerk, C. M. Moysidou, A. J. Boys, A. Withers, R. Vallet and R. M. Owens, Organic electronic transmembrane device for hosting and monitoring 3D cell cultures, *Sci. Adv.*, 2022, **8**(37), eabo4761.
39 K. Oba, K. Ino, Y. Utagawa, H. Abe and H. Shiku, Comprehensive cell adhesion analysis using electrochemiluminescence imaging and electrochemical impedance spectroscopy, *Electrochemistry*, 2024, **92**(2), 022009–022009.
40 A. T. Salminen, Z. Allahyari, S. Gholizadeh, M. C. McCloskey, R. Ajalik, R. N. Cottle, T. R. Gaborski and J. L. McGrath, In vitro studies of transendothelial migration for biological and drug discovery, *Front. Med. Technol.*, 2020, **2**, 600616.
41 J. Yoo, T. H. Kim, S. Park, K. Char, S. H. Kim, J. J. Chung and Y. Jung, Use of elastic, porous, and ultrathin co-culture

membranes to control the endothelial barrier function via cell alignment, *Adv. Funct. Mater.*, 2021, **31**(9), 2008172.

42 M. Hirano, K. Iwata, Y. Yamada, Y. Shinoda, M. Yamazaki, S. Hino, A. Ikeda, A. Shimizu, S. Otsuka, H. Nakagawa and Y. Watanabe, Alveompu: Bridging the gap in lung model interactions using a novel alveolar bilayer film, *Polymers*, 2024, **16**(11), 1486.

43 S. Jalili-Firoozinezhad, F. S. Gazzaniga, E. L. Calamari, D. M. Camacho, C. W. Fadel, A. Bein, B. Swenor, B. Nestor, M. J. Cronce, A. Tovaglieri, O. Levy, K. E. Gregory, D. T. Breault, J. M. S. Cabral, D. L. Kasper, R. Novak and D. E. Ingber, A complex human gut microbiome cultured in an anaerobic intestine-on-a-chip, *Nat. Biomed. Eng.*, 2019, **3**(7), 520–531.

44 Y. Okazaki and T. Katayama, Consumption of non-digestible oligosaccharides elevates colonic alkaline phosphatase activity by up-regulating the expression of IAP-I, with increased mucins and microbial fermentation in rats fed a high-fat diet, *J. Geophys. Res. Oceans*, 2019, **121**(2), 146–154.